EUROPEAN FUSION DEVELOPMENT AGREEMENT

EFDA–JET–CP(01)02-70

R.J.Buttery, T.C.Hender, D.F.Howell, G.T.A.Huysmans, M.Mayoral,
S.D.Pinches, A.Pochelon, O.Sauter, H.Wilson, M.Zabiego
and JET EFDA Contributors

Rotation and Shape Dependence of Neoclassical Tearing Mode Thresholds on JET

Rotation and Shape Dependence of Neoclassical Tearing Mode Thresholds on JET

R.J.Buttery, T.C.Hender, D.F.Howell, G.T.A.Huysmans[1], M.Mayoral,
S.D.Pinches[3], A.Pochelon[2], O.Sauter[2], H.Wilson, M.Zabiego[1]
and JET EFDA Contributors*

Euratom/UKAEA Association, Culham Science Centre, Abingdon, OX14 3EA, UK
[1]Association EURATOM/CEA CEA CADARACHE, DRFC, Bâtiment 513,
13108 Saint-Paul-Lez Durance, France.
[2]CRPP, Association EURATOM-Confédération Suisse, EPFL, 1015 Lausanne, Switzerland.
[3]Max-Planck IPP, IPP-EURATOM Assoziation, Boltzmann-Str.2, D-85748 Garching, Germany.
**See appendix of the paper by J.Pamela "Overview of recent JET results",*
Proceedings of the IAEA conference on Fusion Energy, Sorrento 2000

Preprint of Paper to be submitted for publication in Proceedings of the
EPS Conference,
(Madeira, Portugal 18-22 June 2001)

INTRODUCTION

Neoclassical Tearing Modes (NTMs) may limit performance in the ELMy H-mode regimes in next step devices. NTM physics is complex, not only involving various terms that govern growth of an island, but also dependent on the MHD instability required to 'seed' the island and its coupling to the NTM resonant surface. Thus models have not yet been constrained sufficiently to provide predictive capability [1], and even if this were possible, additional effects in a burning plasmas may change the behaviour further.

Heating systems with low momentum injection, such as ICRH, will reduce differential rotation between seeding perturbations and the NTM resonant surface, where shielding currents initially arise opposing island formation; this could also be an issue for burning plasma devices. With low momentum injection less torque should be needed to lock the seed perturbation to the resonant surface, possibly lowering NTM thresholds. In addition, a route to improve plasma performance is to increase the current carrying capacity of the plasma by application of increased shaping. Thus it is important to study shape effects for ITER.

It is important to study these effects, both to ascertain their likely role in future burning devices, and to test the underlying physics models that will be used to extrapolate to these scales and specify the requirements of the stabilisation systems. In this paper we describe the results of experiments on JET exploring both of these parameters. We consider the implications, and explanation in terms of underlying physics. These studies focus on the m = 3 n = 2 NTM, which is experimentally more accessible on JET, occurring at lower β_N values.

1. ROTATION DEPENDENCE

To explore rotation shear dependence of the NTM thresholds, experiments were performed using slow ramp-up's of total heating power in 1.3MA 1.4T plasmas, where m = 3/n = 2 NTMs are readily triggered in NBI only discharges. The proportion of neutral beam injection (NBI) to ion cyclotron resonant heating (ICRH, 2nd harmonic Hydrogen) was varied between pulses, to provide varying degrees of momentum injection. To minimise the effects of ICRH fast particles, which can stabilise the sawteeth and lower NTM thresholds [2, 3], -90^o phasing was used in an attempt to distribute fast particles outside the core, and minimise effects on sawteeth.

The principal results of the scan are shown in Fig. 1, where degree of momentum injection at time of NTM onset is measured simply by NBI power. There is a pronounced fall in threshold β_N as NBI power (and so momentum injection) is reduced (and ICRH increased). The critical question is whether this is simply due to larger sawteeth with more ICRH? Checking at time of NTM onset shows that sawtooth periods and magnetic amplitudes are actually highest for the high neutral beam cases (Fig 2). A more detailed exploration of time evolutions of discharges shows clearly that there is no significant trend towards larger or longer sawteeth for the higher ICRH proportion discharges at given bN values. Although a slight trend towards high magnetic amplitude is observable with more ICRH, the sawtooth-to-sawtooth scatter is much larger than any systematic variation.

A further question is whether these results are simply due to changes in ion Larmor radius, ρi, which governs the size of the stabilising ion polarisation effect. However, when this affect is corrected for, using previously obtained database fits [4], there is still a clear dependence on level of momentum injection, as in Fig 3.

To conclude, sawtooth variation was minimal during this scan, suggesting the main reason for variation in NTM thresholds is due to changes in momentum injection. This behaviour is akin to studies of error field effects [5], where it is clearly observed (and expected from theory) that increased rotation of a resonant surface with respect to a magnetic perturbation raises the size of perturbation (or torque) required to overcome plasma inertia and drive island formation. The role of differential rotation is highlighted by charge exchange data showing that individual sawteeth reduce differential rotation between q = 1 and q = 1.5 surfaces, sometimes apparently having a cumulative effect on the core rotation. Mode formation usually only occurs as this differential rotation approaches zero. An example of this is shown in Fig 4.

2. SHAPE DEPENDENCE

Various scans in plasma shape have been made with NBI slowly stepped up to determine threshold β_N for NTMs. In a first series of experiments [6] low elongation-low triangularity (termed 'LL') plasmas were compared with high elongation-high triangularity ('HH') cases. Plasma were matched in q_{95} and carefully adjusted in toroidal field and gas puff to ensure similar values of normalised Larmor radius, $\rho_{i\phi}^*$, and normalised collisionality, ν (defined as ion collisionality divided by inverse aspect ratio and electron diamagnetic frequency), at the NTM resonant surface. The resulting plasmas exhibited virtually no difference in β_N thresholds as illustrated for two cases in Fig 4. A further triangularity scan was performed at intermediate elongation to decouple elongation and triangularity effects. The results are shown in Fig 5, where β_N thresholds have been corrected for local parameter variations using previous constant shape database fits for $\rho_{i\phi}^*$ and n dependence [4].

This indicates clear opposing trends with elongation and triangularity. A regression fit yields $\beta_N = 6.4 + 5.9\delta - 3.0\kappa$. However constant $\rho_{i\phi}^*$ and ν is not the appropriate assumption for the operational limit (though useful for exploring the physics trends). In practice, the likely objective of increasing shaping is to increase current carrying capacity at constant toroidal field, B_T, and Greenwald fraction, fGW. Using $\rho_{i\phi}^*$ and ν database fits to scale to constant B_T and f_{GW}, the predicted operational limit due to NTMs can be obtained. Unfortunately, because of large differences in $\rho_{i\phi}^*$ and ν values, the LL and HH pulses (which were generally at higher fields), cannot be sensibly extrapolated, as this procedure is very highly sensitive to the power of ν used, introducing massive uncertainties in predicted values. However the trend for operational NTM limit with triangularity is weakly positive as shown in Fig 7. To understand these results in terms of the underlying physics it is necessary to use the local parameters that occur in the modified Rutherford equation for a growth of an island of size, w:

$$\frac{\tau_r}{r^2}\frac{dw}{dt} = \Delta\text{«}\ \varepsilon^{1/2}(L_q / L_p)\frac{\beta_p}{w}\left(1 - \frac{w^2{}_{pol}}{w^2}\right) \tag{1}$$

given here in terms of tearing stability (Δ'), bootstrap current (β_N/w term), ion polarisation effect ($w_{pol} \approx [g(\nu, \varepsilon)\ (L_q/L_p)\ \varepsilon]^{0.5}\ \rho_{\theta i}$). L_q and L_P are scale lengths, ε measures NTM surface inverse aspect ratio; τ_r, the resistive time scale and ν is normalised collisionality [1]. Growth requires an initial seed, $w = w_{seed} = Aw_{pol}$, where A must be >1, leading to an onset threshold:

$$(L_q / L_p)^{0.5}\ \beta_p = r_s \Delta « \rho_\theta{}^{*} \frac{A}{(1-A^2)}\ \ g(\nu, \varepsilon) \qquad 2)$$

This is plotted in Fig 8, correcting for $(\rho_\theta{}^{*})\ 1.1\ \nu^0$ dependence observed in constant shape scans, to remove effects due to local parameter variations at the resonant surface. Any remaining variation is then expected to be due to the shape influencing the relative seed size, A; the plasma tearing stability; or additional physics terms. However, the trend is puzzling, with some high and low elongation discharges having lower thresholds than the intermediate triangularity scan pulses (triangularity dependence appears weak).

To understand this behaviour we must explore the variation of the various physics ingredients of the NTM equation. Turning first to the seed, studies of sawtooth variation with shape [7] indicate a rapid rise in sawtooth amplitude below k = 1.75, while triangularity effects are weak. Similarly differential rotation between q = 1 and q = 1.5 surface at time of NTM onset in LL pulses is markedly lower than that in HH cases, while variation against triangularity is again weak. Both of these effects would be expected to increase the size of the seed island for LL plasmas (thus lowering the NTM threshold), and are also consistent with the weak dependence seen in the triangularity scan. However, the lower thresholds of the HH cases is harder to understand.

Consideration has also been given to effects of field curvature and variation of the bootstrap drive, using JET-like plasma for calculations of NTM drives. These indicate relatively weak (and opposing) effects of elongation and triangularity in the JET parameter range. Thus the behaviour in local parameters is not fully explained at this time, although further tests are necessary (and planned) to explore additional effects at high elongation, such as a possible reduction in Δ', and test field curvature and bootstrap variation effects in more accurate reconstructions. However the weak triangularity dependence and lowering of thresholds for LL cases seems to be consistent with the trends in underlying physics terms.

CONCLUSIONS.

Studies indicate that NTM thresholds in β_N fall with plasma momentum injection. Checks suggest this is probably not due to variations in sawtooth size, indicating the effect to be primarily related to decreased differential rotation between the sawtooth perturbation and NTM resonant surface, in accordance with a ‘dynamic shielding’ concept. Shape scan experiments, have deconvolved elongation and triangularity effects, and indicate a slight positive trend in the predicted operational limit for ITER with triangularity. The behaviour can largely be understood in terms of underlying physics parameters.

ACKNOWLEDGEMENT

This work has been conducted under the European Fusion Development Agreement, and was partly funded by EURATOM and the UK Department of Trade and Industry.

REFERENCES

[1]. R.J.Buttery et al., Plas. Phys. Contr. Fus. **42** (2000) B61.
[2]. O.Sauter et al., “Neoclassical tearing mode seed island control…”, this conference.
[3]. M.Mantsinen, “ICRF Mode Conversion Experiments on JET”, this conference.
[4]. R.J.Buttery et al., Contr. Fus. and Plas. Phys. (Proc 26 th EPS Maastricht, 1999) **23J** 121.
[5]. E.Lazarro et al., “Rotation effects on error field locked modes…”, this conference.
[6]. R.J.Buttery et al., sec 2 of JET report: JET-R(00)03, UKAEA, OX14 3DB, UK.
[7]. P.C. de Vries et al., “Analysis of shaping effects on sawteeth in JET”, this conference.

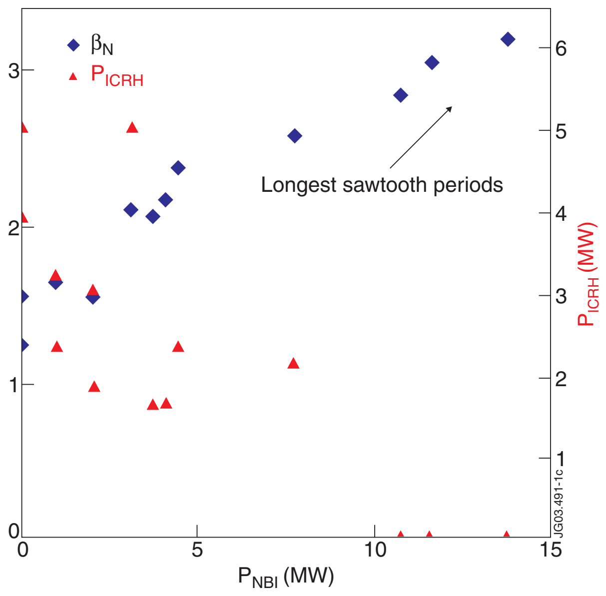

Figure 1: Change in NTM threshold with NBI:RF proportion, vs NBI power.

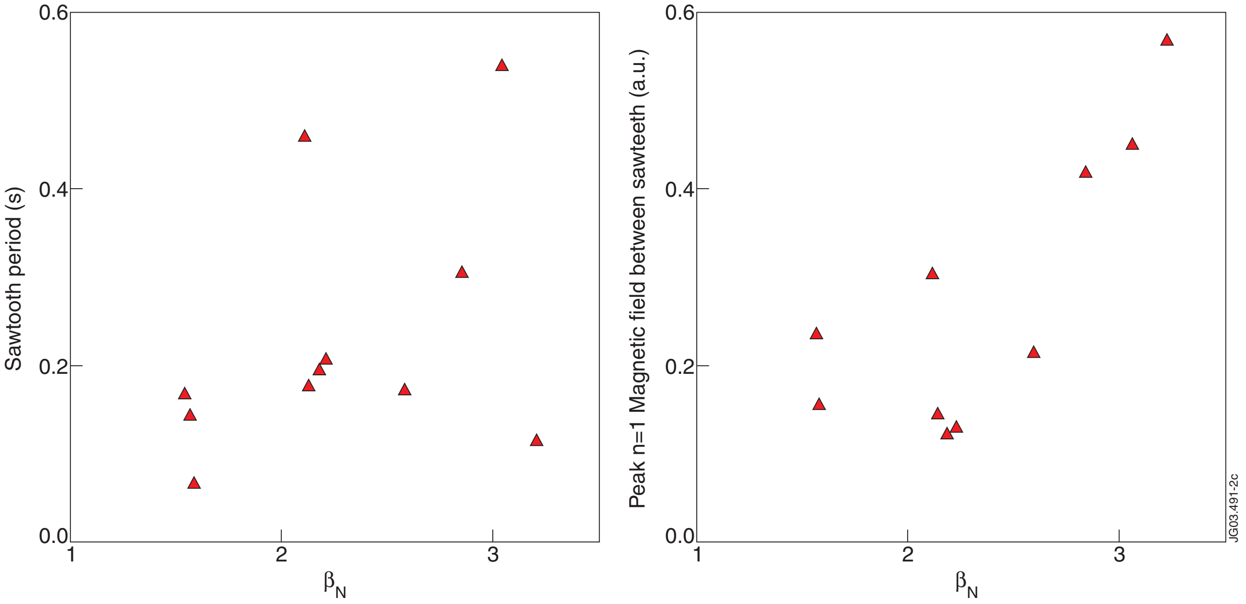

Figure 2: No clear rise in sawtooth period (left) or sawtooth size (right) is observed for low β_N NTM-onset pulses, where more ICRH was used.

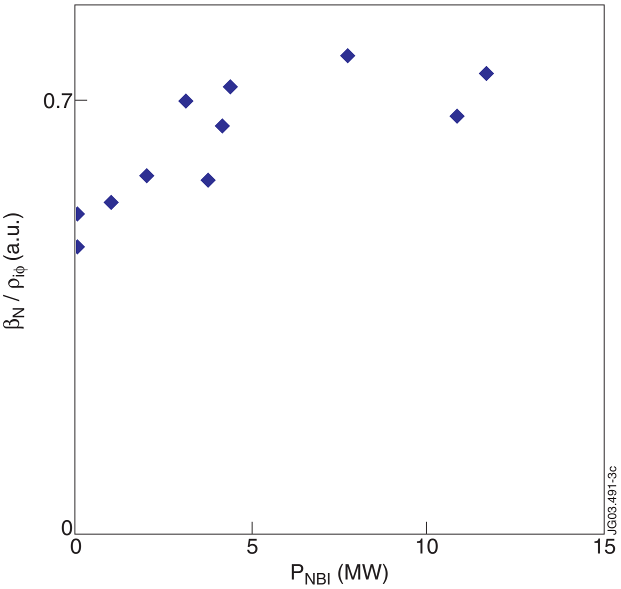

Figure 3: NTM thresholds corrected for Larmor radius variation.

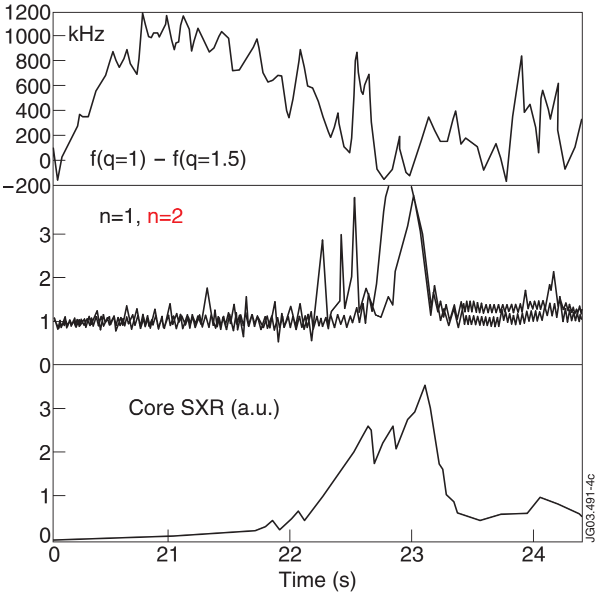

Figure 4: Effect of sawteeth on differential rotation between q = 1 and 1 = 1.5.

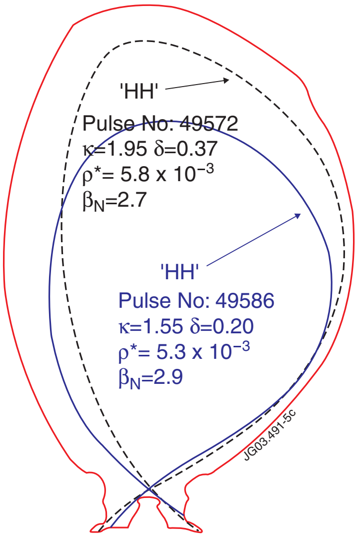

Figure 5: Comparison of LL and HH pulses with NTM onset parameters marked.

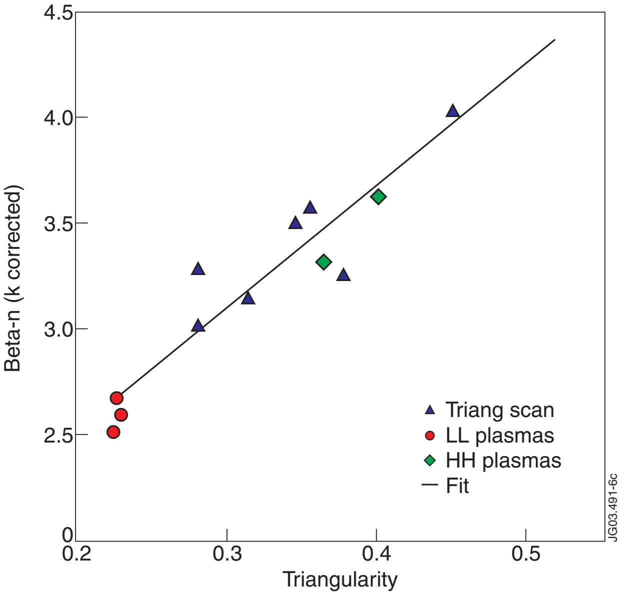

Figure 6: β_N NTM threshold corrected to $\rho^* = 0.006$, $\nu = 0.04$ and elongation.

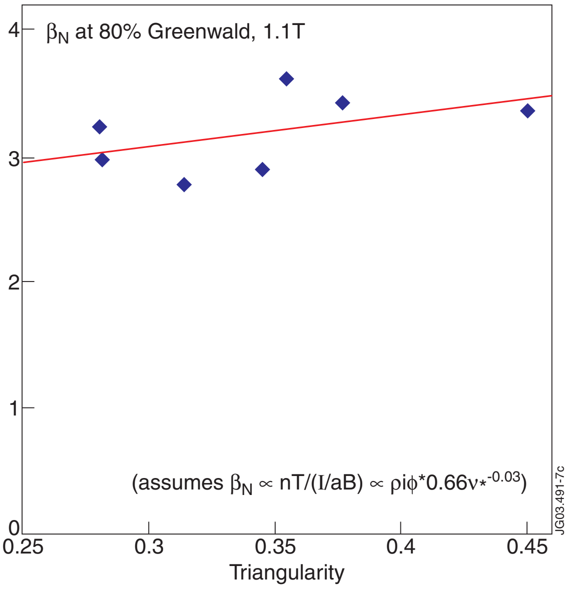

Figure 7: Predicted shape dependence of NTM operational limit at constant B_T and f_{GW}.

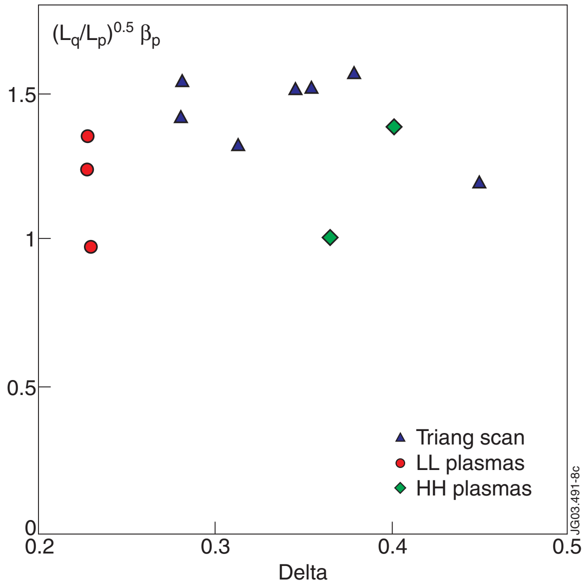

Figure 8: NTM thresholds plotted in 'local' parameters vs triangularity.